Characterizing the Degree of LTE Involvement in Supporting Session Continuity in Street Deployment of NR Systems*

Vyacheslav Begishev[1[0000-0002-7232-4157]],
Andrey Samuylov[1,2[0000-0002-2087-769X]],
Dmitri Moltchanov[2[0000-0003-4007-7187]], and
Konstantin Samouylov[1,3[0000-0002-6368-9680]]

[1] Peoples' Friendship University of Russia (RUDN University), 6 Miklukho-Maklaya St, Moscow, 117198, Russian Federation
[2] Tampere University, Tampere, 33720, Finland
[3] Institute of Informatics Problems, Federal Research Center, "Computer Science and Control" of the Russian Academy of Sciences, 44-2 Vavilova St, Moscow, 119333, Russian Federation
{begishev-vo,samuylov-ak,samuylov-ke}@rudn.ru
{andrey.samuylov, dmitri.moltchanov}@tuni.fi

Abstract. The prospective roll out of recently standardized New Radio (NR) systems operating in millimeter wave frequency band pose unique challenges to network engineers. In this context, the support of NR-based vehicle-to-infrastructure communications is of special interest due to potentially high speeds of user equipment and semi-stochastic dynamic blockage conditions of propagation paths between UE and BR base station (BS). In this conditions even the use of advanced NR functionalities such as multiconnectivity supporting active connections to multiple BSs located nearby may not fully eliminate outages. Thus, to preserve session continuity for UEs located on vehicles a degree of LTE support might be required. In this paper, we quantify the amount of LTE support required to maintain session continuity in street deployment of NR systems supporting multiconnectivity capabilities. Particularly, we demonstrate that it is heavily affected by the traffic conditions, inter-site distance between NR BSs and the degree of multiconnectivity.

Keywords: New Radio, millimeter wave, street deployment, blockage, outage, LTE support, multiconnectivity

* The publication has been supported by "RUDN University Program 5-100" (V.O.Begishev, simulation model development). The reported study was funded by RFBR, project numbers 18-37-00380 (A. Samuylov, numerical analysis) and 18-00-01555 (18-00-01685) (K.E. Samouylov, problem formulation and project administration).

1 Introduction

The New Radio (NR) technology recently standardized by 3GPP promise to bring extraordinary rates at the air interface enabling modern and future rate-greedy applications. However, specifics of propagation properties at millimeter wave frequencies as well as relatively small coverage of such system induces new challenges to system designers.

The problem of dynamic blockage of propagation paths in NR systems has been deeply addressed in recent literature. The models characterizing stochastic properties of blockage and non-blockage intervals under different mobility of UEs and blockers have been reported in [1,2,3]. The authors in [4] employed an analytical representation 3GPP 3D cluster-based propagation model [5] provided in [6] to characterize spatial dependency of channel blockage states.

Identifying outages caused by blockage as one of the main reasons for performance degradation, the authors recently addressed performance of NR systems in dynamic blockage conditions. The upper bound of capacity of NR systems in presence of multiconnectivity is provided in [7]. The practical gains of multiconnectivity with finite number of simultaneously supported links have been reported in [8,9]. The concept of bandwidth reservation to improve session continuity in NR systems has been proposed and analyzed in [10,11]. The joint use of bandwidth reservation and multiconnectivity operation has been assessed in [12,10]. Performance of NR systems in three-dimensional deployments has been assessed in [13,14]. Recently, the studies addressing practical deployments started to appear. Particularly, the study in [15] reports on the NR deployment in square environment. The authors in [16,17] considered complex street deployment of NR systems.

One of the most challenging use-cases for NR system is the support of user equipment (UE) deployed at moving vehicles in street environments. Potentially high speeds of vehicles require frequent BS changes and fast beamalignment procedures. Furthermore, the blockage process is characterized by much coomplex dynamics compared to human bidy blockage that has been thoroughly studies in literature[1,2]. Finally, semi-regular environment, where mobility is limited to straight lanes but the inter-vehicles distance (IVD) and vehicle dimensions are random leads to complex environment for system analysts. As a result, compared to purely stochastic UE deployments such as those observed at squares, parks, leisure resorts, etc., service performance of vehicles in street deployments of NR systems has been loosely characterized so far.

In presence of dynamic vehicle body blockage in street deployment of NR systems, the propagation paths between vehicle-mounted UE and NR base station (BS) can be blocked by other vehicles. Depending on the distance between BS and UE blockage events may lead to outages. To alleviate these consequences of blockage 3GPP has proposed multi-connectivity option [18]. According to it, UE is allowed to support multiple connections to NR BSs located nearly. In case of outage event with the current NR BS, UE may switch one of backup connections. However, the authors in [19] have recently demonstrated that outages may still happen even when three or more connections are simultaneously supported.

One of the critical performance metrics for rate-greedy multimedia applications such as high-definition streaming or augmented/virtual reality, is session continuity. Outage events may produce a drastic negative effect on this metrics causing frequent session interruptions. Thus, to ensure uninterrupted connectivity additional backup radio access technologies such as LTE can be used during outage intervals. In this study, we characterize the required degree of LTE involvement into service process of vehicle-mounted UE in street deployment of NR systems. Introducing *street outage capacity* of NR deployment as the capacity per unit length of a street required by vehicles in outage conditions to support session continuity, we characterize it as a function of (i) street traffic conditions, (ii) degree of multiconnectivity and (iii) inter-site distance (ISD) between BSs. The obtained results can be used to determine the ISD such that LTE BS covering a certain distance of streets in a district may ensure session continuity in case of NR outage conditions.

The rest of the paper is organized as follows. In Section 2 we introduce the system model and metrics of interest. Further, in Section 3 we formalize our performance evaluation framework. We report numerical results in Section 4. The conclusions are drawn in the last section. headings should be numbered. Lower level headings remain unnumbered; they are formatted as run-in headings.

2 System Model

We consider a typical street NR deployment illustrated in Fig. 1. NR BSs are located on both sides of the street, for example, at lampposts that have a constant height h_A. The distance between the access points is such that they form isosceles triangles. The number of lanes is assumed to be $N = 4$. The width of each line is constant and equal to w. We are interested in the UE associated with target vehicle which moves at a speed of v_U. We consider height UE to be constant h_U.

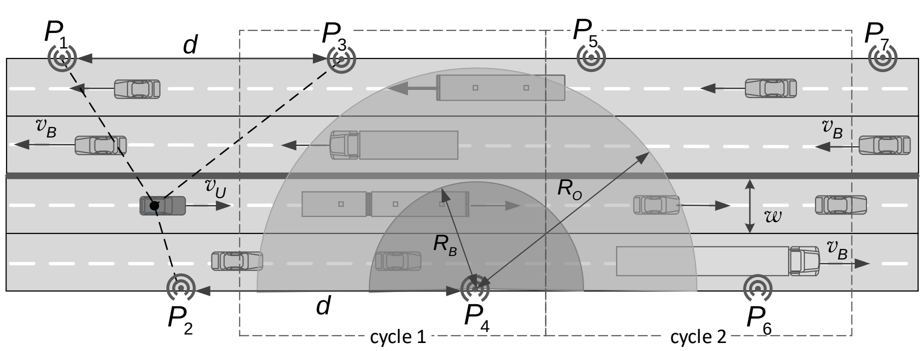

Fig. 1. The considered street NR BS deployment with multi-connectivity operation.

The line-of-sight (LoS) propagation path between NR BS and vehicle-mounted UE may be blocked by moving vehicles, so-called blockers. At each lane blockers form the Poisson process with an intensity λ_B. The vehicle speed is constant and equal to the value v_B. The length of blockers is a random variable characterized by a certain cumulative distribution function (CDF).

In our study, we assume that blockage of LoS by cars leads to a 20 dB decrease in the received signal power. When simulating the NR propagation, we apply the 3GPP urban micro (UMi) street model [5]. According to it, the path loss measured in dB is defined as

$$L(q) = \begin{cases} 52.4 + 21.0 \log q + 20 \log f_c, \text{ blocked}, \\ 32.4 + 21.0 \log q + 20 \log f_c, \text{ non-bl.}, \end{cases} \quad (1)$$

where q is the three-dimensional (3D) distance between the UE and the NR BS, f_c is the carrier frequency in GHz.

The employed propagation model divides the area around NR BS into three zones. In the first zone, limited by distance R_B, no outage may happen regardless of whether LoS is blocked or not. In the second zone, from R_B to R_O, the NR is available if LoS is not blocked. Finally, starting from the distance R_O, no communications is feasible. The values of R_B and R_O are calculated according to the propagation model in (1).

The target UE is allowed to use the 3GPP multi-connectivity operation [18]. According to it, UE maintains an active link with M neighboring NR BSs, where M is known as the "degree of multi-connectivity". We also assume that UE can instantly switch to the best NR BSs out of M available.

Irrespective of the degree of multiconnectivity there might be situations when UE experiences outage with all M available NR BSs. To ensure session continuity we assume that LTE BS located in the area provides additional support. To characterize the degree of LTE involvement into ensuring session continuity, in this study, we concentrate on the so-called *street outage capacity* defined as the bitrate per meter of a street required to ensure session continuity

$$R_O = 4Rp\theta q_i, \quad (2)$$

where is the rate required by vehicle-mounted UE, p is the probability that a vehicle has an active application, $1/\theta$ is the IVD, q_i is the fraction of time in outage conditions when the degree of multiconnectivity is i.

3 System Level Simulation Framework

To quantify the identified metric of interest we have developed a system level simulation framework (SLS) that features analytical pre-processing at the initialization face to speed up the execution. Below, we outline the basic principles of the underlining methodology including the pre-processing phase and actual structure of the simulation engines.

Analyzing the deployment illustrated in Fig.1, one may notice that for a given degree of multiconnectivity M the connectivity patterns itself. Thus, to

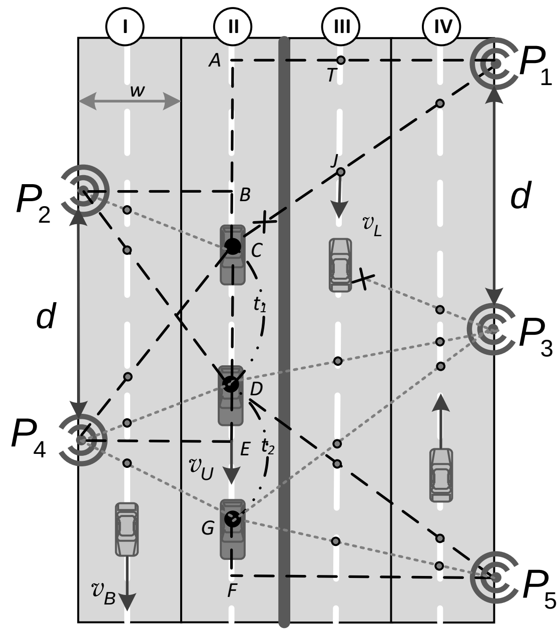

Fig. 2. Detailed illustration of deployment parameters for $M = 3$.

assess the amount of time UE spends in outage conditions, it is sufficient to concentrate on those points in time when the state of UE changes. All these points that define the beginning of different zones can be accurately determined leaving the blocking vehicles and their dimensions as the only stochastic variables. Particularly, for each degree of multiconnectivity, M, we calculate the points of LoS/nLoS state changes. Therefore, before initializing the simulations we first determine the geometry of the zones, where outage may occur, and then proceed with the UE dynamics.

3.1 Analytical Representation

We illustrate the proposed mixed analytical-simulation methodology using $M = 3$ as an example, see Fig. 2. To define the pattern we need to calculate the coordinates of the transition points, C, D, and G, where the set of NR BS associations changes. We denote them as $C(BC, 0, h_U)$, $D(BD, 0, h_U)$, and $G(BG, 0, h_U)$, where the origin is at $B(0, 0, h_U)$. The required distances BC, BD, and BG can be sought from associated triangles.

As an example, consider BC. Using the right triangles $\varDelta P_1AC$ and $\varDelta P_4EC$ and applying the Pythagorean theorem we define the following system:

$$\begin{cases} (P_1A)^2 + (AC)^2 = (P_1C)^2, \\ (P_4E)^2 + (EC)^2 = (P_4C)^2, \\ P_1C = P_4C, \\ AC + EC = 1.5d. \end{cases} \tag{3}$$

Solving the system we arrive at

$$BC = |AC - AB| = |AC - 0,5d|\,. \tag{4}$$

Distances BD and BG are found similarly

$$BD = \frac{(2.5w)^2 + (1.5d)^2 - (1.5w)^2}{3d}, \tag{5}$$

$$BG = \frac{-(2.5w)^2 + (1.5d)^2 + (1.5w)^2}{3d} + 0.5d. \tag{6}$$

Now, the transition points can be written in the general form as

$$x_{n+1} = \frac{(-1)^{n+1}\left[\left(\frac{5w}{2}\right)^2 - \left(\frac{3w}{2}\right)^2\right] + \left(\frac{3d}{2}\right)^2}{3d} + \frac{d(n-1)}{2},\ n = 0, 1, \dots. \tag{7}$$

The latter result can be extended to the case of arbitrary number of lanes $N = 2k$, $k \in \mathbb{Z}$. Particularly, the following provides the locations of the points where the set of UE associations changes

$$x_{n+1} = \frac{(-1)^{n+1}\left[\left(\frac{N+1}{2}w\right)^2 - \left(\left(\left\lfloor\frac{N-1}{2}\right\rfloor + \frac{1}{2}\right)w\right)^2\right]}{3d} + \\ + \frac{(1.5d)^2}{3d} + \frac{d(n-1)}{2},\ n = 0, 1, \dots. \tag{8}$$

Let now t be the time interval a vehicle occludes LoS path. Denote NR BS and UE coordinates by (x_{AP}, y_{AP}, h_A) and (x_{UE}, y_{UE}, h_U), respectively, and coordinates of other vehicles by (x_B, y_B, h_H). To compute t consider triangle $\varDelta P_1AC$. Denote by P_1A a perpendicular from P_1 to a point lying in the middle of the strip of motion. Let this point T have the coordinates (x_T, y_T, z_T). Now, TJ is

$$TJ = \frac{(P_1T)(AC)}{P_1A}, \tag{9}$$

where AC is x-coordinate of the UE, and variables P_1A and P_1T are distances to access point P_1. Observe that the movement in our system is uniformly rectilinear. Thus, TJ and AC for any t are described by the following system

$$\begin{cases} AC = x_A + v_U t, \\ TJ = x_A + v_L t. \end{cases} \tag{10}$$

Using (10) we obtain v_L as

$$v_L = v_U(TJ - x_A)/(AC - x_A). \tag{11}$$

Observe that the time instant t, when two objects moving towards each other meet, is provided by

$$t = \frac{\sqrt{(x_J - x_B)^2 + (y_J - y_B)^2 + (z_J - h_B)^2}}{v_L + v_B}, \tag{12}$$

where (x_J, y_J, z_J) are coordinates of J in Fig. 2

For the cases $M = 1, M = 2$ the analysis is similar.

3.2 Implementation

The simulation engine is built based on time-driven discrete simulation (TD-DES) framework. The software was developed using general-purpose programming language (Java) with multi-threaded optimizations [20]. The modeling procedure consists of two stages, simulation execution and data analysis. The main part of the simulation is to track the initial and final points in time when the marked vehicle is blocked by vehicles moving in other lanes. Each blockage event is processed and stored in an external file. Post-processing of blockage data is then used to determine outage events and their durations.

The following data collection and analysis procedure has been used to obtain the metrics of interest. For each set of input parameters, the simulations were performed for 10^3 seconds of system time. The start of the steady-state period was detected using exponentially-weighted moving average (EWMA) statistics with a weight parameter set to 0.05 [20]. Statistical data were collected in the steady-state only. We used the batch means strategy to remove residual correlations in the statistical data. According to it, the entire data set was divided into 10^5 data blocks. The means of these data blocks served as independent identically distributed observations. Classic statistical methods were further applied to obtain point estimate of the sought metrics of interest.

4 Numerical Results

In this section, we numerically study street outage capacity for a range of system parameters. Particularly, we consider three typical traffic conditions outlined in Table 1. The default system parameters are summarized in Table 2. Also, recalling the structure of expression for street outage capacity in (2), we assume that (i) the unit rate required by an application, $R = 1$ bits/s and (ii) all vehicles are associated with active sessions, i.e., $p = 1$. For non-unit rate R and p, the street outage capacity can be obtained by appropriately scaling the data presented in this section.

Fig. 3 illustrates the street outage capacity as a function of the ISD between NR BSs for $M = 1$, i.e., no multiconnectivity is supported by UEs. As one may

Table 1. Default system parameters.

Scenario	Jam	Normal	Highway
Tagged vehicle speed	20	40	120
Other vehicles speed	20	40	120
Inter-vehicle distance	2	5	20

observe, the street outage capacity remains at the constant level for all considered ISDs for highway traffic conditions. The reason is that the IVD is rather high (20 m.) resulting in rather low density of vehicles per meter. However, as we consider normal traffic conditions the IVD, where IVD is four times smaller while the speed is three times lower, we start to notice differences between street outage capacity for different ISDs. These effects become even more profound when addressing traffic jam conditions. Numerically, for ISD of 100 m $R_O \approx 1.3$ and increases to $R_O \approx 2.2$ for ISD of 600m.

Consider now how the street outage capacity changes when the degree of multiconnectivity increases as indicated in Fig. 4 and Fig. 5. First comparing the results in Fig. 3 and Fig.4 one may notice qunatitative improvement in street outage capacity when swtiching from $M = 1$ to $M = 2$. The most dramatic effect is however, observed for traffic jam road conditions, when the street outage capacity remains almost flat up until approximately 400 m of ISD. Particularly, at ISD of 400 m. operating using just one back up link allows to reduce the amount of traffic that needs to be supported at LTE BS twice. Increasing the degree of multiconnectivity to $M = 3$ allows to decrease LTE requirements even further, especially in the ISD range of $100 - 300$ m. Much milder effect are observed for normal and highway road traffic conditions.

We also would like to specifically highlight the quantitative differences between the amount of traffic that needs to be temporarily supported by LTE technology in different road traffic conditions to ensure session continuity. Par-

Table 2. Default system parameters.

Parameter	Value
Emitted power, P	0.2 W
Carrier frequency, f_C	28 GHz
BS transmit antenna gain, G_T	14.58 dB
UE receive antenna array, G_R	8.57 dB
SNR threshold, S_T	0 dB
Blockage radius in blocked state, R_B	45 m
Outage radius in non-blocked state, R_O	172 m
Height of BS, h_A	5 m
Width of lanes, w	4 m
Number of lanes, N	4
Height of UE, h_U	1.5 m
Mean length of vehicles, L	3.5 m
Mean height of vehicles, h_H	2 m

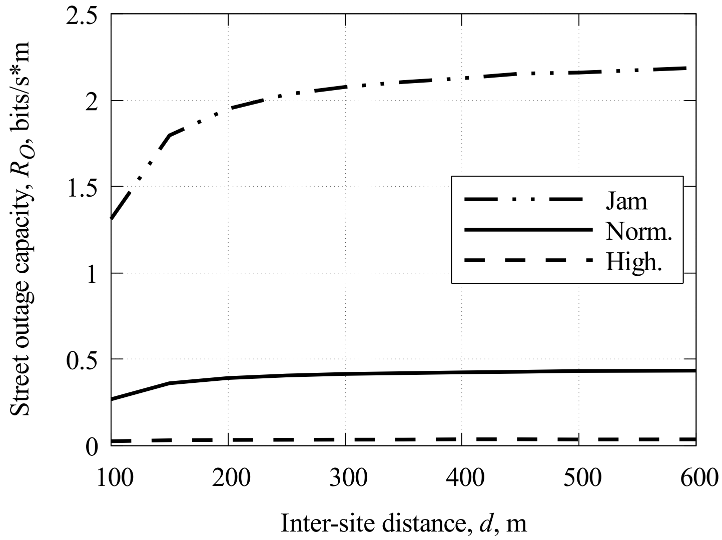

Fig. 3. Street outage capacity, M=1

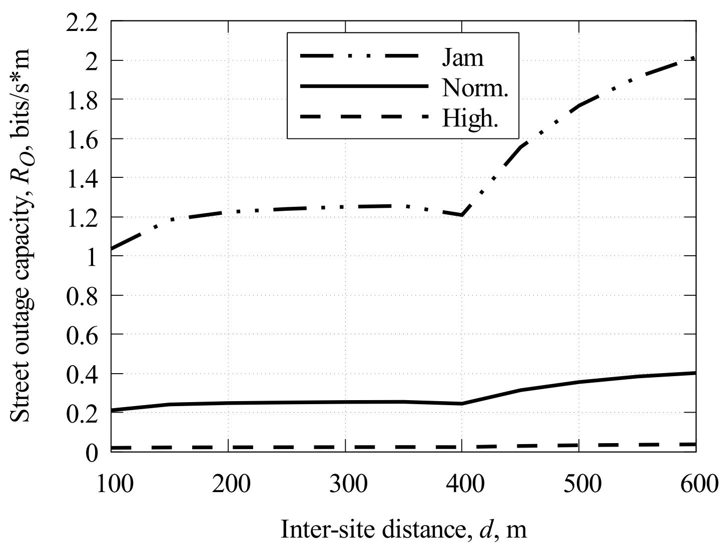

Fig. 4. Street outage capacity, M=2

ticularly, the street outage capacity jam road traffic conditions could be up to four times higher compared to normal conditions inducing large deviations into the amount of traffic that needs to be supported by LTE depending on the time of a day. The mean street outage capacity is highway traffic conditions is usually

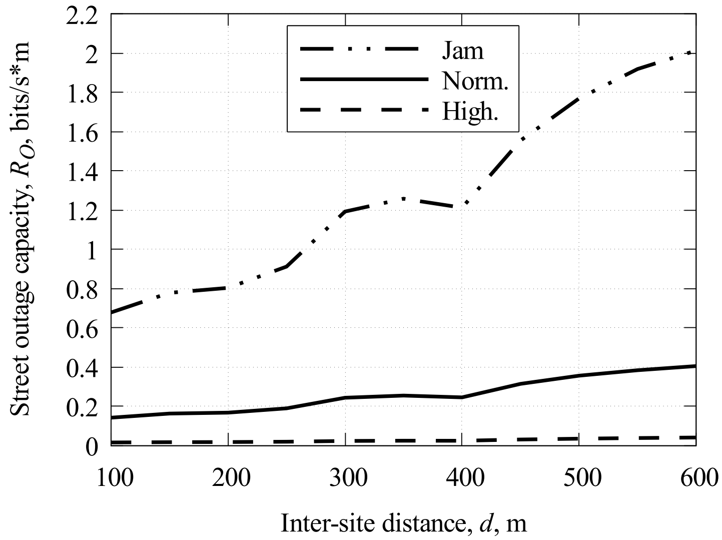

Fig. 5. Street outage capacity, M=3

much smaller even for high ISDs between NR BS allowing to use a single LTE BS to cover large highway segments. These quantitative differences need to be taken into account at the NR deployment phase.

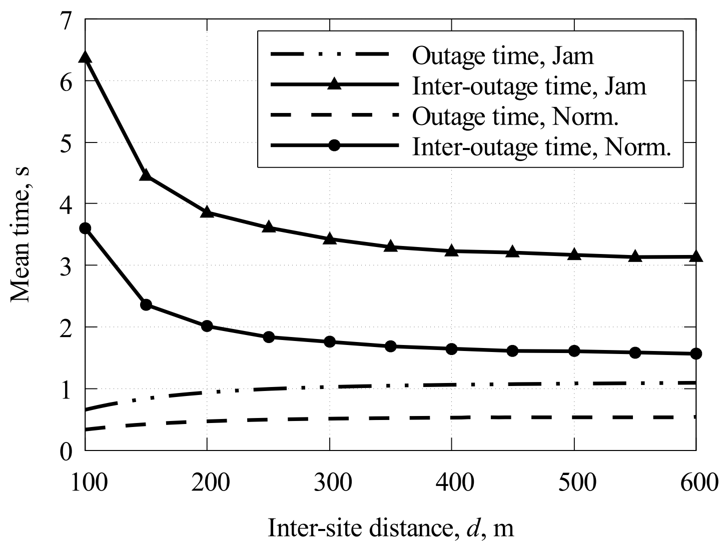

Fig. 6. Mean outage and non-outage time, M=1

Having characterized the street outage capacity we now proceed analyzing the application related performance metrics. Particularly, we concentrate on the mean outage and non-outage times as on the critical metrics for applications. To this end, Fig. 6 – Fig. 8 characterize the outage and non-outage durations as a function of the distance between NR BSs for traffic jam and normal traffic conditions and different degrees of multiconnectivity. Analyzing the results, one may observe that qualitatively the metrics are characterized by similar behavior for all considered values of M. However, the use of higher degree of multiconnectivity drastically decreases the mean outage duration therefore requiring less support from LTE BS.

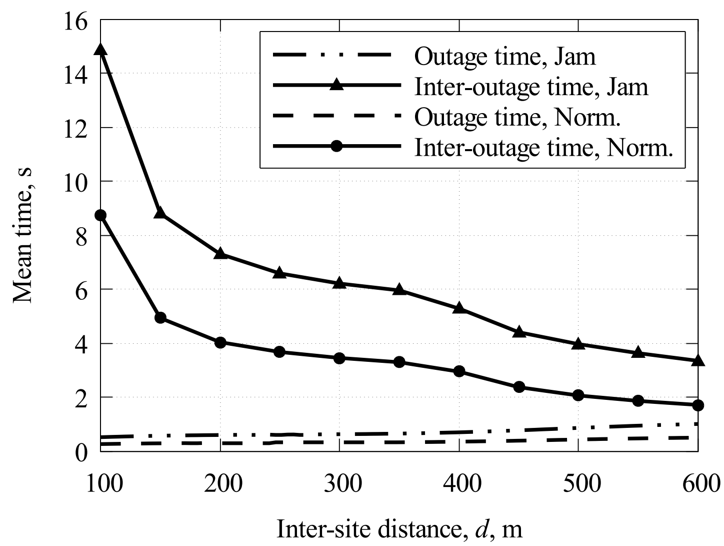

Fig. 7. Mean outage and non-outage time, M=2

One of the important observations that can be deduced from Fig. 6 – Fig. 8 is the intensity of service interruptions caused by outage events. As one may observe, not only the mean durations of outage state increases but the intensity of outage decreases when the the value of M grows.

5 Conclusions

Motivated by ensuring session continuity, in this study we formalized a system model for vehicle-mounted UEs in street deployment of 3GPP NR systems with multiconnectivity capabilities. Having introduced the street outage capacity metric defined as the rate required to ensure session continuity per unit length of a street, we characterized the degree of LTE system involvement in service process of vehicle-mounted UEs.

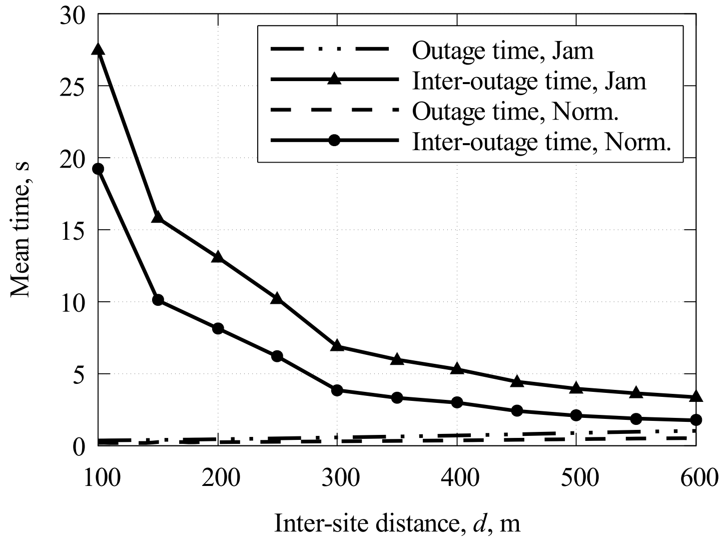

Fig. 8. Mean outage and non-outage time, M=3

Our numerical results indicate that the street outage capacity is drastically affected by the street traffic conditions and the degree of multiconnectivity supported by UE. Particularly, it is mainly affected by inter-vehicle distance and speed of vehicles. Furthermore, the support of multiconnectivity option is vital for traffic jam road conditions as even then use of one back-up link allows to decrease the amount of traffic needed at LTE BSs almost twice. The developed model and presented results can be used to determine the required density of NR BSs such that LTE BS may ensure session continuity in case of outages.

References

1. M. Gapeyenko *et al.*, "On the temporal effects of mobile blockers in urban millimeter-wave cellular scenarios," *IEEE Transactions on Vehicular Technology*, vol. 66, pp. 10124–10138, November 2017.
2. A. Samuylov, M. Gapeyenko, D. Moltchanov, M. Gerasimenko, S. Singh, N. Himayat, S. Andreev, and Y. Koucheryavy, "Characterizing spatial correlation of blockage statistics in urban mmwave systems," in *Globecom Workshops (GC Wkshps), 2016 IEEE*, pp. 1–7, IEEE, 2016.
3. D. Moltchanov, A. Ometov, and Y. Koucheryavy, "Analytical characterization of the blockage process in 3gpp new radio systems with trilateral mobility and multiconnectivity," *Computer Communications*, vol. 146, pp. 110–120, 2019.
4. M. Gapeyenko, A. Samyilov, M. Gerasimenko, D. Moltchanov, S. Singh, M. Akdeniz, E. Aryafar, S. Andreev, and Y. Koucheryavy, "Spatially-consistent human body blockage modeling: A state generation procedure," *IEEE Transactions on Mobile Computing*, vol. 1, no. 1, pp. 1–15, 2019.

5. 3GPP, "Study on channel model for frequencies from 0.5 to 100 GHz (Release 15)," 3GPP TR 38.901 V15.0.0, June 2018.
6. M. Gapeyenko, V. Petrov, D. Moltchanov, S. Andreev, Y. Koucheryavy, M. Valkama, M. R. Akdeniz, and N. Himayat, "An analytical representation of the 3gpp 3d channel model parameters for mmwave bands," in *Proceedings of the 2nd ACM Workshop on Millimeter Wave Networks and Sensing Systems*, pp. 33–38, ACM, 2018.
7. D. Moltchanov, A. Ometov, S. Andreev, and Y. Koucheryavy, "Upper bound on capacity of 5g mmwave cellular with multi-connectivity capabilities," *Electronics Letters*, vol. 54, no. 11, pp. 724–726, 2018.
8. M. Gapeyenko, V. Petrov, D. Moltchanov, M. R. Akdeniz, S. Andreev, N. Himayat, and Y. Koucheryavy, "On the degree of multi-connectivity in 5g millimeter-wave cellular urban deployments," *IEEE Transactions on Vehicular Technology*, vol. 68, no. 2, pp. 1973–1978, 2019.
9. M. Gerasimenko, D. Moltchanov, M. Gapeyenko, S. Andreev, and Y. Koucheryavy, "Capacity of multiconnectivity mmwave systems with dynamic blockage and directional antennas," *IEEE Transactions on Vehicular Technology*, vol. 68, no. 4, pp. 3534–3549, 2019.
10. V. Begishev, D. Moltchanov, E. Sopin, A. Samyilov, S. Andreev, Y. Koucheryavy, and K. Samuilov, "Quantifying the impact of guard capacity on session continuity in 3gpp new radio systems," *IEEE Transactions on Vehicular Technology*, vol. 1, no. 1, pp. 1–15, 2019.
11. D. Moltchanov, A. Samuylov, V. Petrov, M. Gapeyenko, N. Himayat, S. Andreev, and Y. Koucheryavy, "Improving session continuity with bandwidth reservation in mmwave communications," *IEEE Wireless Communications Letters*, vol. 8, no. 1, pp. 105–108, 2018.
12. R. Kovalchukov, D. Moltchanov, V. Begishev, A. Samuylov, S. Andreev, Y. Koucheryavy, and K. Samouylov, "Improved session continuity in 5g nr with joint use of multi-connectivity and guard bandwidth," in *2018 IEEE Global Communications Conference (GLOBECOM)*, pp. 1–7, IEEE, 2018.
13. R. Kovalchukov, D. Moltchanov, A. Samuylov, A. Ometov, S. Andreev, Y. Koucheryavy, and K. Samouylov, "Evaluating sir in 3d millimeter-wave deployments: Direct modeling and feasible approximations," *IEEE Transactions on Wireless Communications*, vol. 18, no. 2, pp. 879–896, 2018.
14. R. Kovalchukov, D. Moltchanov, A. Samuylov, A. Ometov, S. Andreev, Y. Koucheryavy, and K. Samouylov, "Analyzing effects of directionality and random heights in drone-based mmwave communication," *IEEE Transactions on Vehicular Technology*, vol. 67, no. 10, pp. 10064–10069, 2018.
15. V. Petrov, D. Solomitckii, A. Samuylov, M. A. Lema, M. Gapeyenko, D. Moltchanov, S. Andreev, V. Naumov, K. Samouylov, M. Dohler, *et al.*, "Dynamic multi-connectivity performance in ultra-dense urban mmwave deployments," *IEEE Journal on Selected Areas in Communications*, vol. 35, no. 9, pp. 2038–2055, 2017.
16. V. Petrov, M. A. Lema, M. Gapeyenko, K. Antonakoglou, D. Moltchanov, F. Sardis, A. Samuylov, S. Andreev, Y. Koucheryavy, and M. Dohler, "Achieving end-to-end reliability of mission-critical traffic in softwarized 5g networks," *IEEE Journal on Selected Areas in Communications*, vol. 36, no. 3, pp. 485–501, 2018.
17. V. Petrov, D. Moltchanov, S. Andreev, and R. W. Heath Jr, "Analysis of intelligent vehicular relaying in urban 5g+ millimeter-wave cellular deployments," *arXiv preprint arXiv:1908.05946*, 2019.

18. 3GPP, “NR; Multi-connectivity; Overall description (Release 15),” 3GPP TS 37.340 V15.0.0, January 2018.
19. V. Begishev, A. Samuylov, D. Moltchanov, E. Machnev, Y. Koucheryavy, and K. Samouylov, “Connectivity properties of vehicles in street deployment of 3gpp nr systems,” in *2018 IEEE Globecom Workshops (GC Wkshps)*, pp. 1–7, IEEE, 2018.
20. H. G. Perros, “Computer simulation techniques: The definitive introduction!,” 2009.